

# Role of magnetic field in photon excess in heavy ion collisions

Kirill Tuchin

*Department of Physics and Astronomy, Iowa State University, Ames, Iowa 50011, USA*

(Received 30 June 2014; revised manuscript received 18 November 2014; published 14 January 2015)

The synchrotron photon spectrum in heavy ion collisions is computed taking into account the spatial and temporal structure of the magnetic field. It is found that a significant fraction of photon excess in heavy ion collisions in the region  $k_{\perp} = 1\text{--}3$  GeV can be attributed to the synchrotron radiation. Azimuthal anisotropy of the synchrotron photon spectrum is characterized by the Fourier coefficients  $v_2 = 4/7$  and  $v_4 = 1/10$  that are independent of photon momentum and centrality.

DOI: [10.1103/PhysRevC.91.014902](https://doi.org/10.1103/PhysRevC.91.014902)

PACS number(s): 25.75.Cj

## I. INTRODUCTION

One of the outstanding puzzles in the phenomenology of heavy ion collisions is excess of photons at low transverse momenta above the photon spectrum in  $pp$  collisions scaled in proportion to the number of binary nucleon collisions [1]. Another related problem is large azimuthal asymmetry of the photon spectrum [2]. The traditional phenomenological approaches [3–13] have recently improved their agreement with the data, although the discrepancy is not completely eliminated [9,14–17]. A novel mechanism of photon production was proposed in [18]. In [19,20] synchrotron photon radiation by the quark-gluon plasma was investigated and found to give an important contribution to the total photon spectrum. In this paper I go beyond the constant field approximation, employed in [19,20], and compute the synchrotron photon spectrum taking into account the realistic space-time structure of the electromagnetic field.

The electromagnetic field is initially generated by the valance charges of the colliding ions, but at very early times gives way to the induced field generated by the electric currents in the produced matter and travels along with the expanding system [21,22]. The proof of its existence relies only upon the applicability of the effective hydrodynamic description of the final state. Important features of this field are the following: (i) Its strength at time  $t$  is determined only by the collision impact parameter  $b$  and the electrical conductivity  $\sigma$ . It does not explicitly depend on the collision energy. Rather, energy dependence comes through the variation of  $\sigma$  with the temperature  $T$ . (ii) Its dominant component is the magnetic field perpendicular to the event plane [23].

The motion of charged particles of energy  $\varepsilon$  and charge  $e$  in magnetic field  $B$  is quantized, with the distance between the nearby Landau levels being on the order of  $\omega_B = eB/\varepsilon$ . However, if  $eB \ll \varepsilon^2$ , the quantization effect is small. In a thermal medium of temperature  $T$  this condition becomes  $eB \ll T^2$ . The peak strength of the magnetic field at the collision energy  $\sqrt{s_{NN}} = 200$  GeV is estimated to be  $eB = m_{\pi}^2$ , implying that one can treat the synchrotron emission in the quasiclassical approximation. This argument is supported by an explicit calculation in [19], where I showed that the number of Landau levels contributing to the synchrotron radiation at the field strength  $eB = m_{\pi}^2$  is on the order of a hundred.

It is well known that the synchrotron radiation is emitted over a short time  $\Delta t \sim \omega_B^{-1}(m/\varepsilon)^3$  [24], which is much shorter than the characteristic time of the magnetic field variation  $t_B \sim |B/\dot{B}|$ . This allows me to treat the synchrotron radiation as an adiabatic process, viz., to substitute the expression for the time-dependent field (A3) into the emission rate with a constant  $B$ , Eq. (1), which is well known in the literature.

The results of my calculation indicate that, although the synchrotron radiation cannot be responsible for all the observed photon excess, it gives a significant contribution at photon energies  $k_{\perp} = 1\text{--}3$  GeV in the central rapidity region. Since radiation in the direction of the magnetic field vanishes, the synchrotron spectrum exhibits strong azimuthal asymmetry with the following Fourier coefficients:  $v_2 = 4/7$ ,  $v_4 = 1/10$ . This may explain the strong elliptic flow of prompt photons observed in the data [2].

The paper is structured as follows: In Sec. II an analytic expression for the synchrotron spectrum emitted by a relativistic charge is presented. In Sec. III I compute the photon spectrum radiated by the quark-gluon plasma during its entire lifetime using the explicit space-time dependence of magnetic field discussed in the Appendix. The results are shown in Figs. 1, 2, and 3. In Sec. IV the summary is presented.

## II. PHOTON RADIATION BY A RELATIVISTIC QUARK

Consider a relativistic quark or antiquark of energy  $\varepsilon_0$ , velocity  $\mathbf{v}_0$ , and electric charge  $q_f e$  moving in a plane perpendicular to magnetic field  $\mathbf{B}_0$ . I will call the corresponding reference frame  $K_0$ . The emission rate of a photon of energy  $\omega_0$  and momentum  $\mathbf{k}_0 = \omega_0 \mathbf{n}_0$  is given by [25]

$$d\dot{\omega}_0 = \frac{\alpha q_f^2}{(2\pi)^2} \frac{d^3 k_0}{\omega_0} \int_{-\infty}^{+\infty} d\tau \exp \left\{ -\frac{i\varepsilon_0}{\varepsilon'_0} \omega_0 \tau \right. \\ \times \left[ 1 - \mathbf{n}_0 \cdot \mathbf{v}_0 + \left( \frac{q_f e B_0}{\varepsilon_0} \right)^2 \frac{\tau^2}{24} \right] \\ \times \left[ -\frac{\varepsilon_0'^2 + \varepsilon_0^2}{4\varepsilon_0'^2} \left( \frac{q_f e B_0}{\varepsilon_0} \right)^2 \tau^2 - \frac{m^2}{\varepsilon_0 \varepsilon_0'} \right], \quad (1)$$

where  $\varepsilon'_0 = \varepsilon_0 - \omega_0$ .

Consider now another reference frame  $K$  where quarks have an arbitrary direction of momentum. Let the  $y$  axis be in the

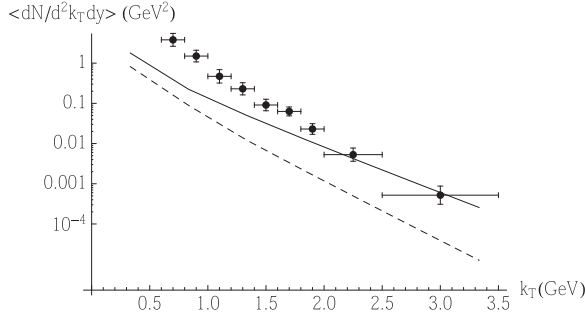


FIG. 1. Spectrum of synchrotron photons averaged over the azimuthal angle versus photon transverse momentum  $k_{\perp}$  at rapidity  $y = 0$  and centrality 0%–20% ( $b = 4.3$  fm [27]). Solid line:  $T = 400$  MeV; dashed line:  $T = 200$  MeV. Data are from [1]; they represent the direct photon  $k_T$  spectra after subtraction of the Ncoll scaled  $p + p$  contribution (Fig. 8 there).

magnetic field direction  $\mathbf{B} = B\hat{y}$  and  $\mathbf{V} = V\hat{y}$  be the velocity of  $K$  with respect to  $K_0$ . Then the Lorentz transformation reads

$$p_{x0} = p_x, \quad 0 = p_{y0} = \gamma(p_y + V\varepsilon), \quad (2)$$

$$p_{z0} = p_z, \quad \varepsilon_0 = \gamma(\varepsilon + Vp_y),$$

$$k_{x0} = k_x, \quad k_{y0} = \gamma(k_y + V\omega), \quad (3)$$

$$k_{z0} = k_z, \quad \omega_0 = \gamma(\omega + Vk_y),$$

$$\mathbf{B}_0 = \mathbf{B}, \quad (4)$$

where  $\gamma = 1/\sqrt{1 - V^2}$ . It follows from the second equation in (2) that

$$V = -\frac{p_y}{\varepsilon} \quad (5)$$

and

$$\varepsilon_0 = \sqrt{\varepsilon^2 - p_y^2}, \quad \omega_0 = \frac{\omega\varepsilon - p_y k_y}{\sqrt{\varepsilon^2 - p_y^2}}. \quad (6)$$

Using the boost invariance of  $k \cdot p$  we get

$$1 - \mathbf{n}_0 \cdot \mathbf{v}_0 = \frac{\omega\varepsilon}{\omega_0\varepsilon_0} (1 - \mathbf{n} \cdot \mathbf{v}), \quad (7)$$

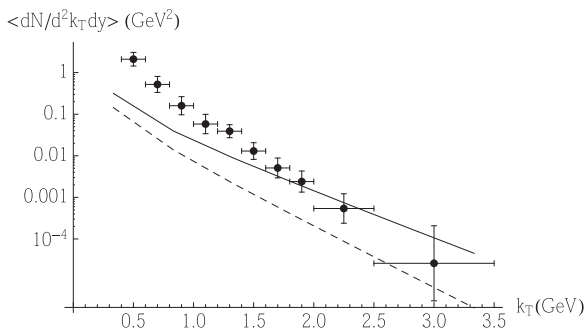


FIG. 2. Spectrum of synchrotron photons averaged over the azimuthal angle versus photon transverse momentum  $k_{\perp}$  at rapidity  $y = 0$  and centrality 40%–60% ( $b = 10.2$  fm [27]). Solid line:  $T = 400$  MeV; dashed line:  $T = 200$  MeV. Data are from [1]; they represent the direct photon  $k_T$  spectra after subtraction of the Ncoll scaled  $p + p$  contribution (Fig. 8 there).

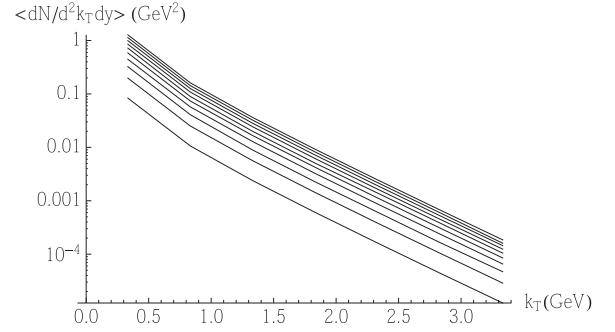


FIG. 3. Time evolution of the photon spectrum (emitted by  $u$  and  $\bar{u}$  quarks) from  $t = 1$  fm (the lowest line) to  $t = 10$  fm (the highest line) in time increments of 1 fm.  $T = 400$  MeV, 0%–20% centrality,  $y = 0$ .

accurate up to the terms of the order  $m^2/\varepsilon^2$ . Transformation of the photon emission rate reads [26]

$$\frac{d\dot{w}}{d\Omega d\omega} = \frac{1}{\gamma^2(1 + V \cos \theta)} \frac{d\dot{w}_0}{d\Omega_0 d\omega_0} = \frac{\omega\varepsilon_0}{\varepsilon\omega_0} \frac{d\dot{w}_0}{d\Omega_0 d\omega_0}, \quad (8)$$

where  $\theta$  is the angle between the photon momentum  $\mathbf{k}$  and the magnetic field, i.e.,  $\cos \theta = n_y$ , and  $\Omega$  is the corresponding solid angle. In the last step I used (5) and (6).  $d\dot{w}_0$  in the right-hand side of (8) is given by (1).

### III. ELECTROMAGNETIC RADIATION BY PLASMA

#### A. Photon rate per unit volume

A quark-gluon plasma in magnetic field radiates photons into a solid angle  $d\Omega$  in the frequency interval  $(\omega, \omega + d\omega)$  with the following rate

$$\frac{dN}{dt d\Omega d\omega} = 2N_c \sum_f \int \frac{d\mathcal{V} d^3p}{(2\pi)^3} f(\varepsilon)[1 - f(\varepsilon')] \frac{d\dot{w}}{d\Omega d\omega}, \quad (9)$$

where  $\mathcal{V}$  stands for the volume, the sum runs over the quark and antiquark flavors and the quark/antiquark distribution function in plasma at temperature  $T$  reads

$$f(\varepsilon) = \frac{1}{e^{\varepsilon/T} + 1}. \quad (10)$$

I introduce now a Cartesian reference frame spanned by three unit vectors  $\mathbf{e}_1, \mathbf{e}_2, \mathbf{n}$ , such that vector  $\mathbf{B}$  lies in the plane spanned by  $\mathbf{e}_1$  and  $\mathbf{n}$ . In terms of the polar and azimuthal angles  $\chi$  and  $\psi$  we can write

$$\mathbf{v} = v(\cos \chi \mathbf{n} + \sin \chi \cos \psi \mathbf{e}_1 + \sin \chi \sin \psi \mathbf{e}_2), \quad (11)$$

$$\mathbf{B} = B(\cos \theta \mathbf{n}_1 + \sin \theta \mathbf{e}_1). \quad (12)$$

Then,

$$p_y = \frac{\mathbf{p} \cdot \mathbf{B}}{B} = \varepsilon v(\cos \chi \cos \theta + \sin \chi \cos \psi \sin \theta), \quad (13)$$

$$k_y = \frac{\mathbf{k} \cdot \mathbf{B}}{B} = \omega \cos \theta, \quad (14)$$

$$\mathbf{n} \cdot \mathbf{v} = v \cos \chi. \quad (15)$$

Quarks moving in plasma parallel to the magnetic field direction do not radiate due to the vanishing Lorentz force. Bearing in mind that at high energies quarks radiate mostly into a narrow cone with the opening angle  $\chi \sim m/\varepsilon$ , we conclude that photon radiation at angles  $\theta \lesssim m/\varepsilon$  can be neglected. Thus, expanding at small  $\chi$  we obtain from (6) and (13)

$$\varepsilon_0 \approx \varepsilon \sin \theta, \quad \omega_0 \approx \omega \sin \theta, \quad \theta > \frac{m}{\varepsilon}. \quad (16)$$

Omission of terms of order  $m/\varepsilon$  is consistent with the accuracy of (1). In view of (16), dependence of the integrand of (9) on angle  $\chi$  comes about only in (7), viz.,

$$1 - \mathbf{n}_0 \cdot \mathbf{v}_0 = \frac{1}{\sin^2 \theta} \left( 1 - \cos \chi + \frac{m^2}{2\varepsilon^2} \right), \quad (17)$$

while it is  $\psi$  independent.

To integrate over the quark/antiquark momentum directions  $do = d \cos \chi d\psi$  we write (9) as

$$\begin{aligned} \frac{dN}{dt d\Omega d\omega} &= \frac{2N_c}{(2\pi)^3} \sum_f \int d\mathcal{V} \int_\omega^\infty d\varepsilon \varepsilon^2 f(\varepsilon) [1 - f(\varepsilon')] \\ &\times \int do \frac{d\dot{w}}{d\Omega d\omega}, \end{aligned} \quad (18)$$

substitute (8) and (1), and integrate first over  $do$  and then over  $\tau$  with the following result (see details in [25]):

$$\begin{aligned} &\int do \frac{d\dot{w}_T}{d\Omega d\omega} \\ &= -\frac{\alpha q_f^2 m^2}{\varepsilon^2} \sin^2 \theta \left\{ \int_{z_\theta}^\infty \text{Ai}(z') dz' + (\sin \theta)^{2/3} \left( \frac{\varepsilon}{\varepsilon'} \right)^{1/3} \right. \\ &\quad \left. \times \left( \frac{\omega_B}{\omega} \right)^{2/3} \frac{\varepsilon^2 + \varepsilon'^2}{m^2} \text{Ai}'(z_\theta) \right\}, \end{aligned} \quad (19)$$

where  $\omega_B = q_f e B / \varepsilon$  and

$$z_\theta = \left( \frac{\varepsilon}{\varepsilon'} \right)^{2/3} \left( \frac{\omega}{\omega_B} \right)^{2/3} \frac{m^2}{\varepsilon^2 \sin^{8/3} \theta}. \quad (20)$$

### B. Photon spectrum

Spatial and temporal dependence of the photon production rate (18) comes about from the corresponding dependence of the background magnetic field. The explicit form of the magnetic field is given in the Appendix. Neglecting small variations of magnetic field strength in the transverse plane, integration over the time and volume of plasma yields the total photon multiplicity spectrum radiated into a unit solid angle,

$$\begin{aligned} \frac{dN}{d\Omega d\omega} &= \frac{2N_c}{(2\pi)^3} S \sum_f \int_0^{t_f} dt \int_{-t}^t dz \int_\omega^\infty d\varepsilon \varepsilon^2 f(\varepsilon) [1 - f(\varepsilon')] \\ &\times \int do \frac{d\dot{w}}{d\Omega d\omega}, \end{aligned} \quad (21)$$

with (A3) substituted into (19) and (20), and the overlap area  $S$  of two spherical nuclei of radius  $R_A$  given by

$$S = R_A^2 [2 \arccos(b/2R_A) - \sin(2 \arccos(b/2R_A))]. \quad (22)$$

The experimental observable is the photon multiplicity at a given transverse momentum  $k_\perp$ , azimuthal angle  $\phi$ , and rapidity  $y$  with respect to the collisions axis. It reads

$$\frac{dN(k_\perp, \phi, y)}{k_\perp dk_\perp d\phi dy} = \frac{dN(\omega, \theta)}{\omega d\omega d\Omega}, \quad (23)$$

where  $\omega = k_\perp \cosh y$  and  $\cos \theta = \sin \phi / \cosh y$ . It is usually represented as the cosine Fourier series

$$\frac{dN(k_\perp, \phi, y)}{k_\perp dk_\perp d\phi dy} = \left\langle \frac{dN}{d^2 k_\perp dy} \right\rangle_\phi \left( 1 + \sum_{n=1}^{\infty} 2v_n \cos(n\phi) \right), \quad (24)$$

where the azimuthally averaged multiplicity is given by

$$\left\langle \frac{dN}{d^2 k_\perp dy} \right\rangle_\phi = \frac{1}{2\pi} \int_0^{2\pi} \frac{dN}{d^2 k_\perp dy} d\phi, \quad (25)$$

and the ‘‘flow’’ coefficients by

$$v_n = \frac{1}{2\pi} \int_0^{2\pi} \frac{dN}{d^2 k_\perp dy} \cos(n\phi) d\phi \left\langle \frac{dN}{d^2 k_\perp dy} \right\rangle_\phi^{-1}. \quad (26)$$

In Figs. 1 and 2 I display the spectrum of synchrotron plasma radiation over time  $t \leq t_f = 10$  fm at different temperatures and centralities. The values of temperature are chosen as two extremes for which the synchrotron spectrum is still consistent with the data and physics of the QGP. One can see that at low  $k_\perp$  synchrotron photons cannot account for the bulk of the photon excess. However, they contribute a substantial fraction of photons at  $k_\perp = 2-3$  GeV. We also conclude that the data favors temperatures below  $T = 400$  MeV.

Figure 3 shows the time evolution of the photon spectrum. It is interesting to note that although the spectrum grows fastest at early times it is still increasing even near the freeze-out time  $t_f$ . This is because the photon spectrum is proportional to  $B^{2/3}$  [see (27)] while the magnetic field decreases as  $B \sim 1/t^2$ , so that the spectrum is proportional to  $1/t_f^{1/3}$ . It seems to me that taking into account the time dependence of plasma temperature and conductivity will lead to a faster decrease of the photon emission rate with time, as can be inferred from (27).

Concerning the Fourier coefficients (26), the ones with odd indexes vanish,  $v_{2k+1} = 0$ ,  $k = 0, 1, 2, \dots$ , while the ones with even indexes  $v_{2k}$  rapidly decrease with increase of  $k$ . Two largest coefficients are  $v_2 = 0.57$  and  $v_4 = 0.10$ . They turned out to be independent of  $k_\perp$  and centrality. I will explain this behavior in the next subsection. Here I would like to note that, in view of the results shown in Figs. 1 and 2, a large elliptic flow of photons observed in [2] seems to be at least partially due to the strong azimuthal asymmetry of the synchrotron radiation, which is in turn a consequence of the  $\mathbf{v} \times \mathbf{B}$  form of the Lorentz force. The above values of  $v_2$  and  $v_4$  that indicate large anisotropy of synchrotron protons should not be directly compared to experiment, but rather should be included in an average over many different sources of azimuthal anisotropy in the photon spectrum.

### C. Photon spectrum at high $k_{\perp}$

Analytical expressions for the photon spectrum can be found for photons with  $k_{\perp} \gg T$ , which in fact applies to most of the phenomenologically relevant photons. In this limit we approximate  $f(\varepsilon) \approx e^{-\varepsilon/T}$  and  $z_{\theta} \ll 1$ . Keeping in (21) only the leading terms in  $z_{\theta}$  and neglecting  $m$  compared to  $T$  we obtain

$$\frac{dN}{d^2k_{\perp}dy} = \alpha \frac{2N_c}{(2\pi)^3} \frac{\Gamma(2/3)}{3^{1/3}\Gamma(1/3)} (\sin\theta)^{8/3} e^{-k_{\perp}/T} T^{2/3} \times \sum_f \int dV \int_0^{t_f} dt (q_f eB)^{2/3}. \quad (27)$$

Substituting into (25) we derive for the average photon multiplicity

$$\left\langle \frac{dN}{d^2k_{\perp}dy} \right\rangle_{\phi} = \alpha \frac{2N_c}{(2\pi)^3} \frac{\Gamma(11/6)}{3 \times 6^{1/3}\Gamma(7/6)\Gamma(7/3)} e^{-k_{\perp}/T} T^{2/3} \times \sum_f \int dV \int_0^{t_f} dt (q_f eB)^{2/3}, \quad (28)$$

while the Fourier coefficients follow from (26)

$$v_2 = \int_{-\pi/2}^{\pi/2} \cos(2\phi)(\cos\phi)^{8/3} d\phi \Big/ \int_{-\pi/2}^{\pi/2} (\cos\phi)^{8/3} d\phi = \frac{4}{7}, \quad (29)$$

$$v_4 = \int_{-\pi/2}^{\pi/2} \cos(4\phi)(\cos\phi)^{8/3} d\phi \Big/ \int_{-\pi/2}^{\pi/2} (\cos\phi)^{8/3} d\phi = \frac{1}{10}. \quad (30)$$

Equation (28) gives a reasonable approximation for the high- $k_{\perp}$  tail of the photon spectrum. Especially striking is the agreement between (29) and (30) and the values of  $v_2$  and  $v_4$  cited in the previous subsection. Apparently, the dominant contribution to the azimuthal angle integration arises at high  $k_{\perp}$ . This fact then explains independence of the Fourier coefficients on  $k_{\perp}$ ,  $T$ ,  $B$ , and other parameters.

### IV. CONCLUSIONS

In this paper I computed the synchrotron photon spectrum in heavy ion collisions taking into account the spatial and temporal structure of the magnetic field. Results obtained in this paper indicate that a significant fraction of photon excess in heavy ion collisions in the region  $k_{\perp} = 1-3$  GeV can be attributed to the synchrotron radiation. Azimuthal anisotropy is characterized by the ‘‘flow’’ coefficients  $v_2 = 4/7$  and  $v_4 = 1/10$  that are independent of photon momentum and centrality. Although synchrotron photons alone cannot account neither for the total photon spectrum, nor for its azimuthal asymmetry, they nevertheless give an important contribution to both. In my opinion, any comprehensive description of photons produced in heavy-ion collisions must include a contribution of synchrotron radiation.

Throughout the paper I assumed that plasma temperature and electrical conductivity are time independent, which

allowed me to use the analytical expressions for the magnetic field, (A1)–(A3). This approach should give a rather accurate estimate of the photon spectrum because time variation of temperature and electrical conductivity is rather mild. For example, in the Bjorken scenario  $\sigma, T \propto t^{-1/3}$  [28]. Nevertheless, a more accurate approach should incorporate a realistic flow of plasma; see, e.g., [29,30].

### ACKNOWLEDGMENTS

I would like to thank Sanshiro Mizuno for providing the experimental data. This work was supported in part by the US Department of Energy under Grant No. DE-FG02-87ER40371.

### APPENDIX: MODEL FOR MAGNETIC FIELD IN HEAVY ION COLLISIONS

An analytic expression for the electromagnetic field created in heavy ion collisions is found in [21,22]. It is a sum over  $Z$  point charges moving in the positive  $z$  direction and  $Z$  point charges moving in the opposite direction. Equations simplify in the relativistic limit  $\gamma\sigma b \gg 1$ . In this case the magnetic field created at the origin by a point charge  $e$  moving along the positive  $z$  axis at transverse distance  $b$  reads

$$\mathbf{B} = \frac{e}{2\pi} \hat{\phi} \left( \frac{\gamma b}{2(b^2 + \gamma^2 t^2)^{3/2}} + \frac{b\sigma}{4t^2} e^{-\frac{b^2\sigma}{4t}} \right). \quad (A1)$$

The first term in the bracket is the boosted Coulomb field in vacuum, while the second term is the field induced in the medium. The quark-gluon system is released from the nuclear wave functions by  $t \sim 1/Q_s \sim 0.2$  fm, where  $Q_s$  is the saturation momentum. By that time the Coulomb term is negligible so that the field in the medium is determined only by  $b$  and  $\sigma$ . Therefore, the total magnetic field is given by

$$\mathbf{B} = \frac{e}{2\pi} \left[ \theta(t-z) \sum_{a=1}^Z \frac{\sigma(\mathbf{b}/2 - \mathbf{b}_a)}{4(t-z)^2} e^{-\frac{\sigma(\mathbf{b}/2 - \mathbf{b}_a)^2}{4(t-z)}} + \theta(t+z) \sum_{a=1}^Z \frac{\sigma(\mathbf{b}/2 - \mathbf{b}_a)}{4(t+z)^2} e^{-\frac{\sigma(\mathbf{b}/2 - \mathbf{b}_a)^2}{4(t+z)}} \right], \quad (A2)$$

where  $\mathbf{b}_a$ 's are the proton transverse coordinates,  $\mathbf{b}$  is the impact parameter,  $z$  is the longitudinal position,  $\theta$  is a step function, and  $\alpha = e^2/4\pi$  is the fine structure constant. At large  $Z$  the magnetic field (A2) is approximately isotropic in the  $xy$  plane (i.e., in the plane transverse to the collision axis) and can be well described by the following model:

$$\mathbf{B} = \frac{eZ}{2\pi} \hat{\mathbf{y}} \left[ \theta(t-z) \frac{\sigma(R_p + b/2)}{4(t-z)^2} e^{-\frac{(R_p + b/2)^2\sigma}{4(t-z)}} + \theta(t+z) \frac{\sigma(R_p + b/2)}{4(t+z)^2} e^{-\frac{(R_p + b/2)^2\sigma}{4(t+z)}} \right]. \quad (A3)$$

Quantum uncertainty of a proton position is accounted for by a finite parameter  $R_p = 1$  fm [31].

- [1] A. Adare *et al.* (PHENIX Collaboration), [arXiv:1405.3940](#).
- [2] A. Adare *et al.* (PHENIX Collaboration), [Phys. Rev. Lett.](#) **109**, 122302 (2012).
- [3] E. V. Shuryak, [Phys. Lett. B](#) **78**, 150 (1978); [Yad. Fiz.](#) **28**, 796 (1978) [[Sov. J. Nucl. Phys.](#) **28**, 408 (1978)].
- [4] R. C. Hwa and K. Kajantie, [Phys. Rev. D](#) **32**, 1109 (1985).
- [5] J. Kapusta, P. Lichard, and D. Seibert, [Phys. Rev. D](#) **44**, 2774 (1991); **47**, 4171 (1993).
- [6] R. Baier, H. Nakkagawa, A. Niegawa, and K. Redlich, [Z. Phys. C](#) **53**, 433 (1992).
- [7] P. B. Arnold, G. D. Moore, and L. G. Yaffe, [J. High Energy Phys.](#) 11 (2001) 057.
- [8] P. B. Arnold, G. D. Moore, and L. G. Yaffe, [J. High Energy Phys.](#) 06 (2002) 030.
- [9] H. van Hees, C. Gale, and R. Rapp, [Phys. Rev. C](#) **84**, 054906 (2011).
- [10] S. Turbide, C. Gale, E. Frodermann, and U. Heinz, [Phys. Rev. C](#) **77**, 024909 (2008).
- [11] H. Holopainen, S. S. Räsänen, and K. J. Eskola, [Phys. Rev. C](#) **84**, 064903 (2011).
- [12] S. A. Bass, B. Muller, and D. K. Srivastava, [Phys. Rev. Lett.](#) **93**, 162301 (2004).
- [13] P. Aurenche, M. Fontannaz, J. P. Guillet, B. A. Kniehl, E. Pilon, and M. Werlen, [Eur. Phys. J. C](#) **9**, 107 (1999).
- [14] O. Linnyk, W. Cassing, and E. L. Bratkovskaya, [Phys. Rev. C](#) **89**, 034908 (2014).
- [15] C. Shen, U. W. Heinz, J.-F. Paquet, and C. Gale, [Phys. Rev. C](#) **89**, 044910 (2014).
- [16] R. Chatterjee, H. Holopainen, I. Helenius, T. Renk, and K. J. Eskola, [Phys. Rev. C](#) **88**, 034901 (2013).
- [17] R. Chatterjee, H. Holopainen, T. Renk, and K. J. Eskola, [Phys. Rev. C](#) **83**, 054908 (2011).
- [18] G. Basar, D. E. Kharzeev, and V. Skokov, [Phys. Rev. Lett.](#) **109**, 202303 (2012).
- [19] K. Tuchin, [Phys. Rev. C](#) **87**, 024912 (2013).
- [20] K. Tuchin, [Phys. Rev. C](#) **83**, 017901 (2011).
- [21] K. Tuchin, [Adv. High Energy Phys.](#) **2013**, 490495 (2013).
- [22] K. Tuchin, [Phys. Rev. C](#) **88**, 024911 (2013).
- [23] D. E. Kharzeev, L. D. McLerran, and H. J. Warringa, [Nucl. Phys. A](#) **803**, 227 (2008).
- [24] L. Landau and E. Lifshitz, *The Classical Theory of Fields*, Course of Theoretical Physics. Vol. 2, 4th ed. (Butterworth-Heinemann, Oxford, 1980).
- [25] V. B. Berestetsky, E. M. Lifshitz, and L. P. Pitaevsky, *Quantum Electrodynamics*, Course of Theoretical Physics Vol. 4 (Pergamon, Oxford, 1982), Sec. 90, p. 652.
- [26] K. Tuchin, [Phys. Rev. C](#) **88**, 024910 (2013).
- [27] D. Kharzeev and M. Nardi, [Phys. Lett. B](#) **507**, 121 (2001).
- [28] J. D. Bjorken, [Phys. Rev. D](#) **27**, 140 (1983).
- [29] L. McLerran and V. Skokov, [arXiv:1305.0774](#).
- [30] B. G. Zakharov, [Phys. Lett. B](#) **737**, 262 (2014).
- [31] A. Bzdak and V. Skokov, [Phys. Lett. B](#) **710**, 171 (2012).